CIVIL ENGINEERING JOURNAL

Article no. 20

THE CIVIL ENGINEERING JOURNAL 2-2022

RESEARCH ON THE PREDICTION OF RIGID FRAME-CONTINUOUS GIRDER BRIDGE DEFLECTION USING BP AND RBF NEURAL NETWORKS

Liu Jingyang, Wu Hexiang and Sun Quansheng

Department of Civil Engineering, Northeast Forestry University, Harbin，150040, China; 1258362856@qq.com; whx2015@nefu.edu.cn; sunquansheng@nefu.edu.cn

ABSTRACT

To solve the problem of excessive deflection in the post-operation process of a rigid frame-continuous girder bridge and provide a basis for the setting of its initial camber, this paper, based on the results of finite element analysis, uses three methods to predict and verify the deflection of a rigid frame-continuous girder bridge. The results show that the average deflection method can be used to fit the average deflection value for a relatively long period of time and predict the average deflection value for the next longer period of time. Both the back-propagation (BP) neural network model and the radial basis function (RBF) neural network model can predict deflection well, but the RBF neural network model has higher prediction accuracy, with a mean absolute error (MAE) of 2.55 $x10^{-5}$ m and a relative error not exceeding 1%. The prediction model established by the RBF neural network has higher stability, better generalization ability, and better overall prediction performance. The established model has some reference significance for similar engineering projects and can achieve the optimization of structural parameters.

KEYWORDS

Rigid frame-continuous girder bridge, BP neural network, RBF neural network, Deflection prediction, Structural parameter optimization

INTRODUCTION

Current status of research

With the advancement of transportation and building technology, highway construction has expanded into hilly regions. The severe terrain characteristics, such as high mountains, deep ravines, and steep slopes, increase the prevalence of rigid frame-continuous girder bridges with tall piers and extended spans. Typically, rigid frame-continuous girder bridges are constructed using the cantilever-symmetrical casting method, which is influenced by a number of variables, and the variation of internal forces and displacements is very complex. With the increasing service life of rigid frame-continuous girder bridges constructed with cantilever casting, it has been discovered that the mid-span deflection of these bridges is generally too great, or even cracking is observed, which not only severely affects the use and safety of the bridges but also limits the development and breakthrough of this bridge type to larger spans. To ensure that the bridge can be closed normally, that the bridge line shape and stress meet the design specifications, and that the structure is safe, it is necessary to monitor and control the deformation, stress, and safety during the construction process, thereby accurately predicting the mid-span deflection. Currently, the most popular approaches for making predictions include the least-squares method, the gray system theory, the Kalman filtering method, the artificial neural network method, etc. Since the influencing parameters of the construction of rigid frame continuous girder bridges, such as volume weight of concrete, elastic modulus, concrete shrinkage and creep, and temperature load, are subject to random

variations, artificial neural networks have been rapidly developed in recent years as an integral part of the rapidly developing artificial intelligence. Neural networks, as a technique for nonlinear data modelling, may rapidly determine the functional relationship between input parameters and output parameters [10]. Recently, academics have become interested in the optimization of construction-related factors using neural networks. The two most commonly employed neural networks are BP (back propagation) and RBF (radial basis function). The BP network is a multi-layer feedforward network trained using error backpropagation with an input layer, a hidden layer, and an output layer [11]. During backpropagation, the weights and offsets are changed continuously to bring the actual output of the network closer to the expected output [12]. The alteration of weights and offsets influences the output of the BP network; hence, the BP neural network is a "universal approximation" of the nonlinear mapping [13]. The RBF neural network has a similar structure to the BP neural network, but the input parameters are directly transferred to the hidden layer without weight connections, and the radial basis function is used as the neuron activation function for the hidden layer[14]. Non-linear is the transformation from the input layer to the hidden layer, whereas linear is the transformation from the hidden layer to the output layer [15]. It has the "local mapping" attribute since the output of the RBF network is only dependent on a few adjustment factors. In light of this issue, this work applies the average deflection approach for a single-factor deflection prediction analysis on a bridge with a rigid frame continuous girder bridge that is currently under construction. A rigid frame-continuous girder bridge deflection prediction model is developed utilizing a BP neural network and an RBF neural network. In order to optimize structural characteristics and advance construction control technology, the prediction results are compared and studied in order to select the approach with the highest prediction accuracy and greatest effect.

Engineering overview and finite element modeling

The background of this paper is a rigid-continuous beam bridge, which is a prestressed concrete semi-rigid-continuous box beam bridge with a span of (70 + 120 + 70) m and a cantilever casting construction method. The total length of the bridge is 1046 meters. The total width of the bridge deck is 11.5 meters (anti-collision guardrail). The transverse slope of the bridge deck is 1.5% in both directions. The design speed is 80 kilometers per hour, the vehicle load grade is highway-I standard, and the design safety level is one level.

Using Midas/Civil, the finite element model of the underpinning engineering was developed. The model construction stage was segmented based on the engineering design documents and adjusted in real time based on the actual construction situation on the job site. The construction of the model was divided into twelve stages.

The primary bridge consists of 127 distinct nodes and 122 simplified units. The pier beams are simulated by beam elements, with rigid connections between the 18-foot main beam and the main pier and elastic connections between the 19-foot seat beam and the main beam. The section and material parameters are selected based on the bridge's design document and modified based on field measurements. Given that the bridge is cast using the cantilever method, the bracket is simulated using node general support (only compression); the corresponding finite element model is depicted in Figure 1.

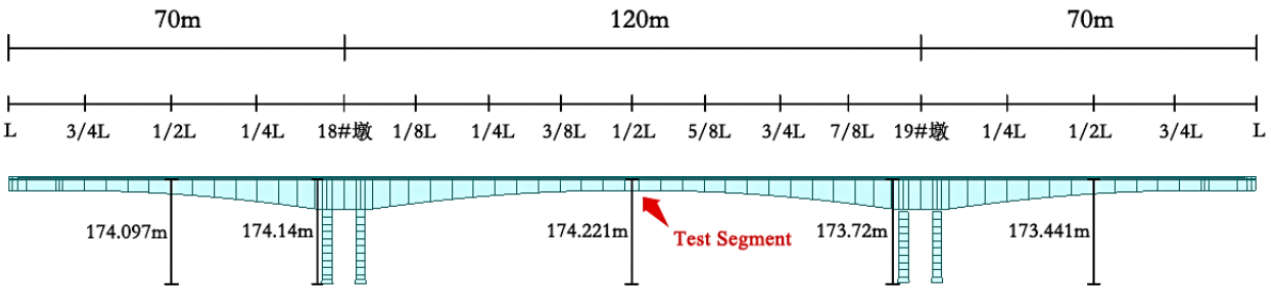

Fig. 1 – Graph of the Finite Element Model

METHODS

Analysis of single-factor deflection prediction

In this section, the measured deflection values at the 1/4L position of the second span of Pier 18, based on the engineering dependency, from late August 2022 to early January 2023, are selected. The deflection data is then fitted and predicted using the least squares method. Divide each month into two periods (every 15 days is one period), calculate the average measured deflection value of the two periods, create a new sample point, fit the sample of the first five months (1~10 periods) using the least squares method, and use the sample of the sixth month (11~12 periods) to predict deflection. The average mean value of deflection (AMVOD), the minimum value of deflection (mVOD) and the maximum value of deflection (MVOD) are shown in Table 1. The line graph of the measured average deflection is depicted in Figure 2.

Using Matlab software and the principle of least squares [16], the relationship between the average value of the mid-span deflection f (mm) and the time (period) can be fitted by a third-order polynomial.

$$f = 0.00929t^3 - 0.1725\ t^2 + 0.01547\,t - 1.186 \quad (1)$$

Where f is the Average deflection and t represents The number of periods. Each month is divided into two halves, one each in the first and second halves. Figure 3 depicts the deflection's fitting curve. The fitting curve is close to the average value of the measured deflection between the measured deflection minimum curve and the measured deflection maximum curve, and it has a high degree of fitting.

Tab. 1 - Measured average deflection table

Numbers	Time	AMVOD/m	mVOD/m	MVOD/m
1	Aug.16th-30th	-1.36 x10^{-3}	1.06 x10^{-3}	-3.78 x10^{-3}
2	Sept.1st-15th	-1.735 x10^{-3}	0.74 x10^{-3}	-4.21 x10^{-3}
3	Sept.16th-30th	-2.43 x10^{-3}	0.32 x10^{-3}	-5.18 x10^{-3}
4	Oct.1st-15th	-3.27 x10^{-3}	-0.52 x10^{-3}	-6.02 x10^{-3}
5	Oct.16th-30th	-4.465 x10^{-3}	-1.82 x10^{-3}	-7.11 x10^{-3}
6	Nov.1st-15th	-5.13 x10^{-3}	-2.87 x10^{-3}	-7.39 x10^{-3}
7	Nov.16th-30th	-5.92 x10^{-3}	-3.31 x10^{-3}	-8.53 x10^{-3}
8	Dec.1st-15th	-7.885 x10^{-3}	-5.81 x10^{-3}	-9.96 x10^{-3}
9	Dec.16th-30th	-8.335 x10^{-3}	-6.32 x10^{-3}	-1.035 x10^{-2}
10	Jan.1st-15th	-8.925 x10^{-3}	-6.47 x10^{-3}	-1.138 x10^{-2}
11	Jan.16th-30th	-9.18 x10^{-3}	-7.47 x10^{-3}	-1.089 x10^{-2}
12	Feb.1st-15th	-9.97 x10^{-3}	-7.93 x10^{-3}	-1.201 x10^{-2}

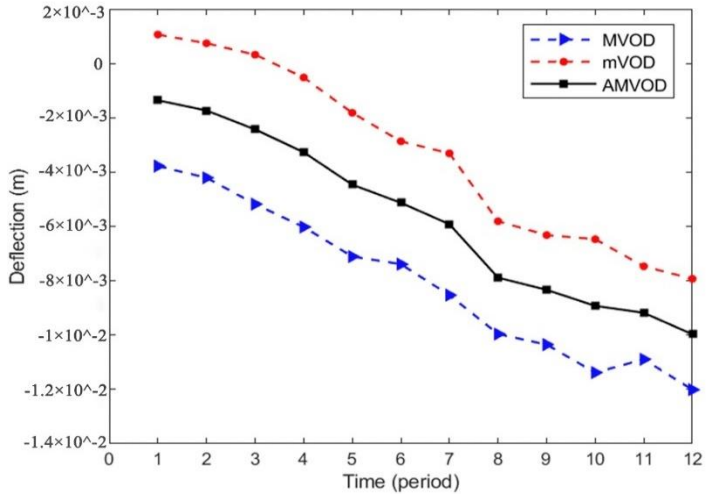

Fig. 2 – The line graph of the measured average deflection

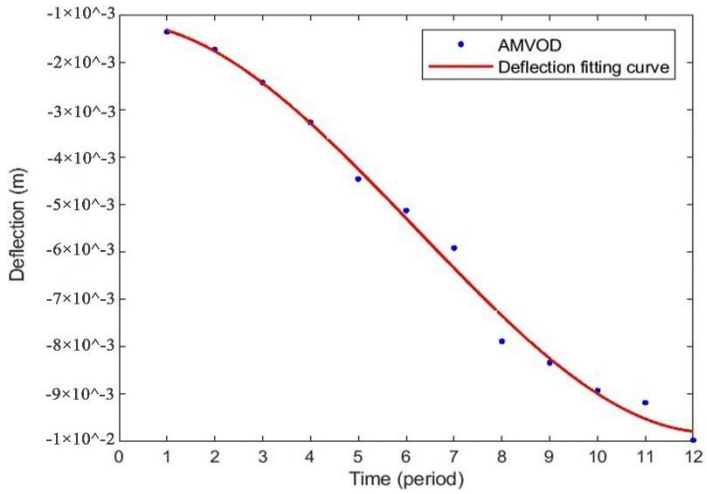

Fig. 3 – Diagram of the deflection fitting curve

Table 2 depicts the relative error between the measured average deflection and the fitted value for the first five months, i.e. the first through tenth period.

Tab. 2 - Relative error fitting deflection

Numbers	Measured Value/m	Predicted Value/m	Relative Error/%
1	-1.360 x10^{-3}	-1.334 x10^{-3}	1.91
2	-1.735 x10^{-3}	-1.771 x10^{-3}	2.07
3	-2.430 x10^{-3}	-2.441 x10^{-3}	0.45
4	-3.270 x10^{-3}	-3.290 x10^{-3}	0.61
5	-4.465 x10^{-3}	-4.260 x10^{-3}	4.59
6	-5.130 x10^{-3}	-5.297 x10^{-3}	3.26
7	-5.920 x10^{-3}	-6.344 x10^{-3}	7.16
8	-7.885 x10^{-3}	-7.346 x10^{-3}	6.84
9	-8.335 x10^{-3}	-8.247 x10^{-3}	1.06
10	-8.925 x10^{-3}	-8.991 x10^{-3}	0.74

The predicted deflection values for the sixth month, i.e. the 11th and 12th periods, are -9.523 x10^{-3} m and -9.787 x10^{-3} m, which are close to the measured values of -9.180 x10^{-3} m and -9.970 x10^{-3} m, indicating that the prediction model is accurate. The relative error between measured and predicted values is displayed in Table 3.

Tab. 3 - Prediction relative error of deflection

Numbers	Measured Value/m	Predicted Value/m	Relative Error/%
11	-9.180 x10^{-3}	-9.523 x10^{-3}	3.74
12	-9.970 x10^{-3}	-9.787 x10^{-3}	1.84

The above calculation demonstrates that the average deflection method can be used to fit the average deflection value over a longer time period and predict the average deflection value over the next longer time period.

Analysis of multi-factor deflection prediction

Experimental program

In order to ensure that the experiment is effective and to examine the influence of elastic modulus, volume weight of concrete, concrete shrinkage strain, and temperature load on deflection, elastic modulus (EM), volume weight of concrete (VWOC), material age (MG), and minimum temperature (MT) are used as input variables. Based on the calculation results of the Midas/Civil finite element model. The EM is set to 3.53x10^{4}MPa~3.57x10^{4}MPa; the VWOC is 23KN/m^3~27KN/m^3; the MG is 5~9 days; and the MT is -51℃~-55℃. The four factors and five levels are coded according to Table 4. During the construction process, the tensioning of prestressed tendons exerts an upward force on the beam segment, causing it to lift. As time progresses, the deflection of the beam segment also gradually increases. In this study, the deflection of the beam segment after the prestressing of segment 12 of Pier 18, measured using Midas/Civil software, was used as the evaluation criterion. Based on the data in Table 4, a single-factor control variable method was employed to investigate the influence of parameters on the deflection of the main beam. Twenty sets of experiments were designed as training samples, as shown in Table 5. Twenty sets of experiments were designed as training samples. As shown in Table 6, eight sets of experiments are designed as test verification based on the experiment's general principle. The experimental flowchart is depicted in Figure 4.

Tab. 4 - Structure parameter factor coding level table

Numbers	EM/MPa	VWOC/(KN/m^3)	MG/days	MT/°C
1	3.53x10^4	23	5	-51
2	3.54x10^4	24	6	-52
3	3.55x10^4	25	7	-53
4	3.56x10^4	26	8	-54
5	3.57x10^4	27	9	-55

Tab. 5 - Training samples

Numbers	EM/MPa	VWOC/(KN/m^3)	MG/days	MT/°C	Deflection/m
1	3.53x10^4	23	9	-55	2.8730 x10^{-2}
2	3.54x10^4	23	9	-55	2.8660 x10^{-2}
3	3.55x10^4	23	9	-55	2.8600 x10^{-2}
4	3.56x10^4	23	9	-55	2.8530 x10^{-2}
5	3.57x10^4	23	9	-55	2.8472 x10^{-2}
6	3.57x10^4	23	9	-55	2.8472 x10^{-2}
7	3.57x10^4	24	9	-55	2.6929 x10^{-2}
8	3.57x10^4	25	9	-55	2.5387 x10^{-2}
9	3.57x10^4	26	9	-55	2.3844 x10^{-2}
10	3.57x10^4	27	9	-55	2.2302 x10^{-2}
11	3.57x10^4	23	5	-55	2.8474 x10^{-2}
12	3.57x10^4	23	6	-55	2.8474 x10^{-2}
13	3.57x10^4	23	7	-55	2.8473 x10^{-2}
14	3.57x10^4	23	8	-55	2.8473 x10^{-2}
15	3.57x10^4	23	9	-55	2.8472 x10^{-2}
16	3.57x10^4	23	9	-51	2.9199 x10^{-2}
17	3.57x10^4	23	9	-52	2.9017 x10^{-2}
18	3.57x10^4	23	9	-53	2.8835 x10^{-2}
19	3.57x10^4	23	9	-54	2.8654 x10^{-2}
20	3.57x10^4	23	9	-55	2.8472 x10^{-2}

Tab. 6 - Testing samples

Numbers	EM/MPa	VWOC/(KN/m^3)	MG/days	MT/°C	Deflection/m
1	3.55x10^4	24	9	-55	2.7049 x10^{-2}
2	3.55x10^4	24	5	-55	2.7051 x10^{-2}
3	3.55x10^4	25	7	-55	2.5500 x10^{-2}
4	3.55x10^4	25	9	-55	2.5499 x10^{-2}
5	3.55x10^4	26	5	-55	2.3952 x10^{-2}
6	3.55x10^4	26	7	-55	2.3951 x10^{-2}
7	3.55x10^4	27	5	-55	2.2402 x10^{-2}
8	3.55x10^4	27	7	-55	2.2401 x10^{-2}

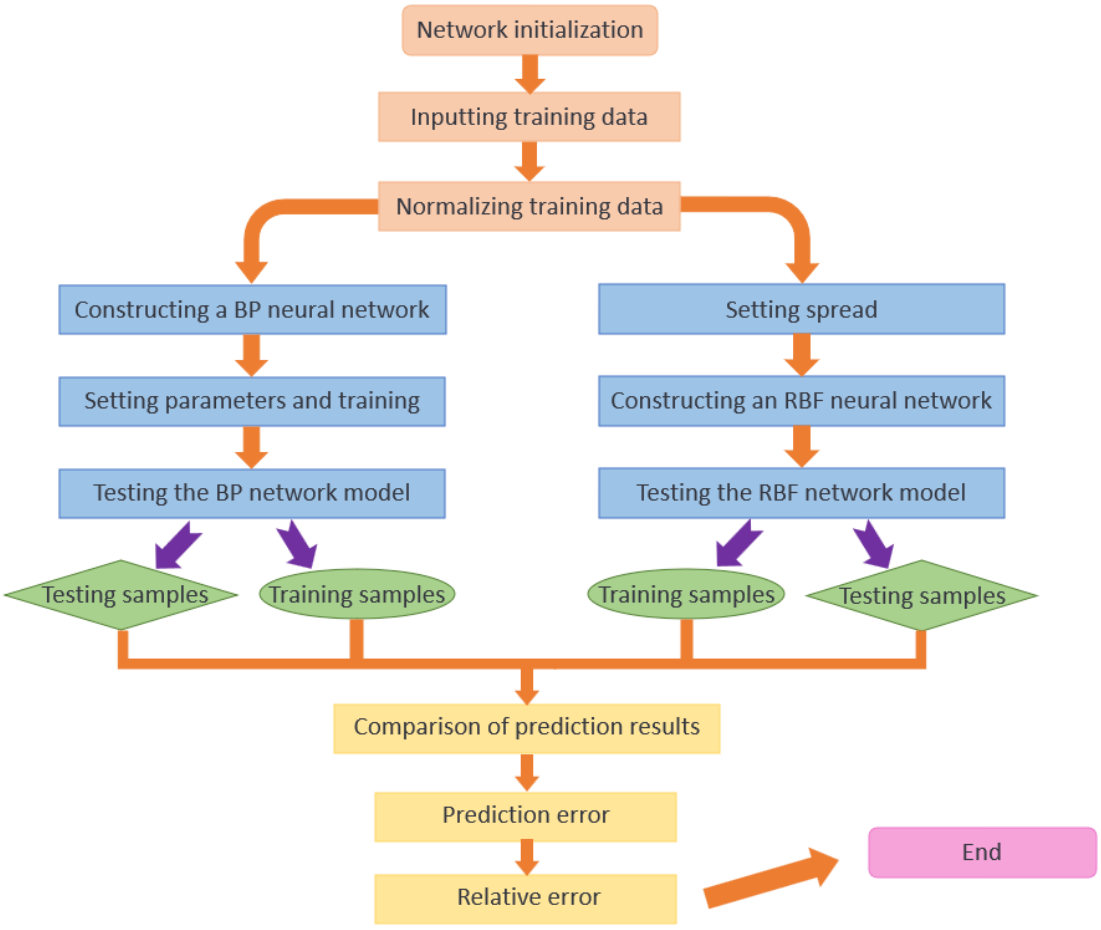

Fig. 4 – Experimental flowchart

BP neural network model construction

A three-layer BP neural network is used to establish a prediction model, with elastic modulus (EM), volume weight of concrete (VWOC), material age (MG), and minimum temperature (MT) as input variables and deflection value as output. Therefore, the constructed neural network model has 4 nodes in the input layer and 1 node in the output layer. The BP neural network is a multi-layer feed-forward network trained by error backpropagation, which consists of an input layer, a hidden layer, and an output layer. By continuously modifying the weights and offsets, the actual output of the network is closer to the desired output. The model operation feeds back the output results to the output layer through backpropagation of the input variables (EM, VWOC, MG, MT) so as to obtain the output result, that is, the deflection prediction value, and the number of nodes in the hidden layer is also One of the key factors affecting the BP neural network model is that if there are too many nodes in the hidden layer, it will increase the network training time, and it is easy to overfit during the training process. If the number of nodes in the hidden layer is small, the neuron training is insufficient and cannot achieve. The intended target of the network. In this study, the mean square value of the error is aimed at, and the optimal number of neurons in the hidden layer is mainly obtained through trial and error. After repeated training, when the number of nodes in the hidden layer is 4, the mean square value of the error is the smallest, and the prediction performance of the BP neural network is the best. Using 28 sets of experimental data samples for analysis, the data were normalized so that the model sample data fell between [0, 1], and the function used was following:

$$xi = (x - min(xi))/(max(xi) - min(xi)) \quad (2)$$

Where he normalized data is xi, where $min(xi)$ and $max(xi)$ are, respectively, the smallest and largest numbers in the data. The training samples from the experimental data are used to construct the prediction model, while the test samples are used to evaluate the model's generalization ability. The hidden layer transfers functions "tansig" and "purelin" are selected, and the training function "trainlm" is selected. Using the newff function, a neural network model is created. Maximum training time is 400 seconds, target mean square error is 0.001, and learning rate is 0.05. The model is trained and validated to obtain prediction results.

RBF neural network model construction

The RBF neural network is similar to the BP neural network in structure, but it uses radial basis functions as activation functions for the hidden layer neurons. The input parameters are directly mapped to the hidden layer without requiring weight connections. The output of the RBF network is only dependent on a subset of adjustable parameters, making it possess the characteristic of "local mapping". Using an RBF neural network to normalize 28 sets of data and then develop a prediction model, the number of input and output nodes is the same as that of the BP neural network, but the number of hidden layer nodes achieved a better approximation effect with 20 neurons. Build a neural network model using the "newrbe" function. In the RBF neural network model, the expanding coefficient has a significant impact on the RBF model's prediction accuracy. After multiple trials, it is set to 1, the mean square error target is set to 0.001, and experimental data is trained and evaluated.

RESULTS

To validate the prediction performance of BP and RBF neural network models, the fitting degree of the two network models was compared, and the fitting regression of the sample values and the model training output values on the training samples and test samples was obtained, as depicted in Figure 5. The fitting correlation coefficients for the two network models are all up to 0.99, indicating a high degree of fit to the training samples. When the normalized sample value equals the training value of the model, that is, when the fitting line Y=T, the fitting correlation coefficient (R) value is 1. The greater the correlation between the actual output and the expected output, the closer the R value is to 1. On the test sample, the BP neural network model's fitting correlation coefficient is 0.97507, and the predicted output deviates from the target output. The RBF neural network model has an appropriate correlation coefficient of 0.9991. Based on the preceding analysis, it is clear that both network models have good prediction capabilities, but the RBF neural network outperforms the other in terms of prediction accuracy for the input sample.

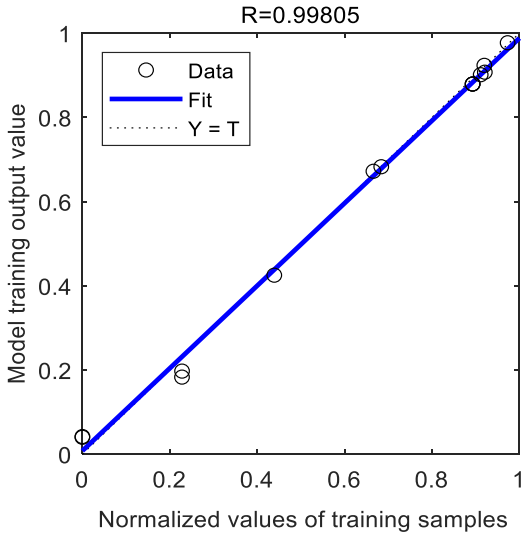

(a) Training samples of BP network

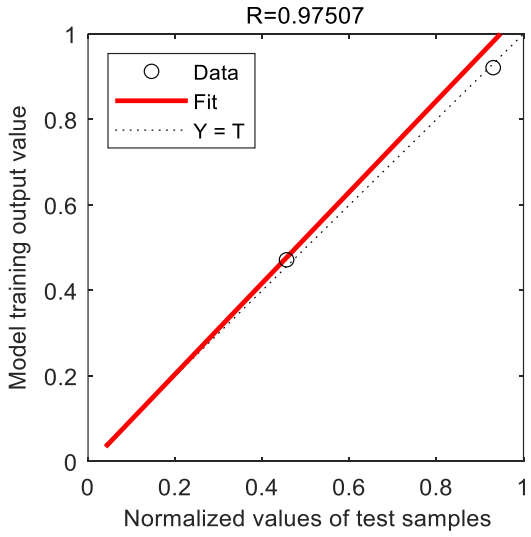

(b) Testing samples of BP network

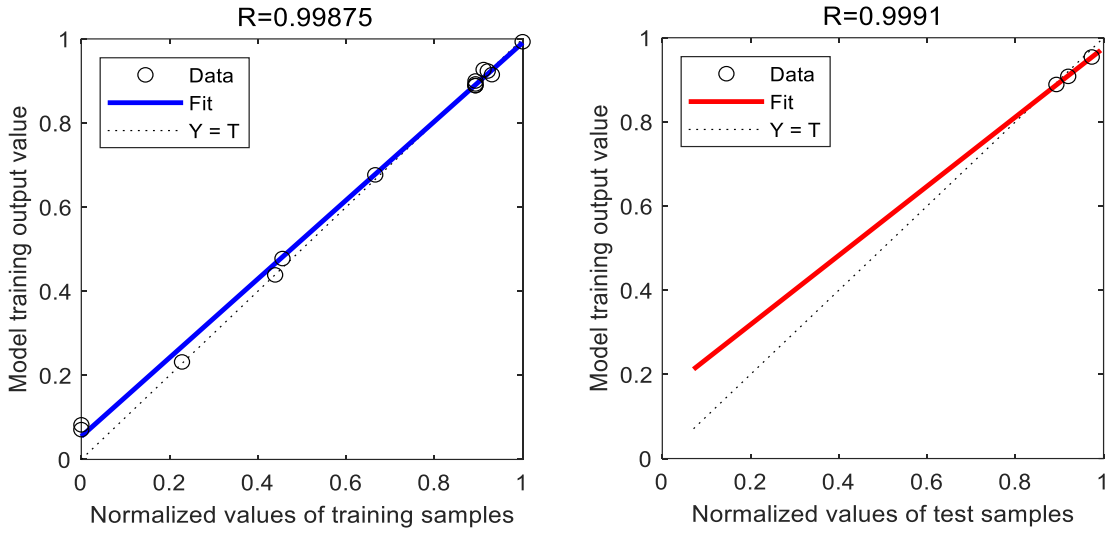

(c) Training samples of RBF network *(d) Testing samples of RBF network*

Fig. 5 – The prediction and fitting curves of BP and RBF neural network models' performance

To further validate the prediction performance, the BP and RBF neural network models were developed to predict the deflection, and the normalized output values of the deflection on training samples and test samples were obtained, as depicted in Figure 6. For the training samples, the predicted values of the BP and RBF constructed network models are essentially consistent with the actual values, and both neural network models do an excellent job of approximating the samples. Although there is a certain amount of error when comparing the test samples to the predicted samples, the overall prediction effect is good, and the predicted deflection falls within the acceptable error range. As shown in the figure, the BP neural network has a higher prediction accuracy only in the seventh group of test samples, and the prediction result is superior to that of the RBF neural network but inferior to that of the RBF neural network in the other groups of test samples. The root mean square error (RMSE) of the RBF neural network is significantly smaller than that of the BP neural network, indicating that the RBF neural network has a smaller deviation between the predicted value and the actual value.

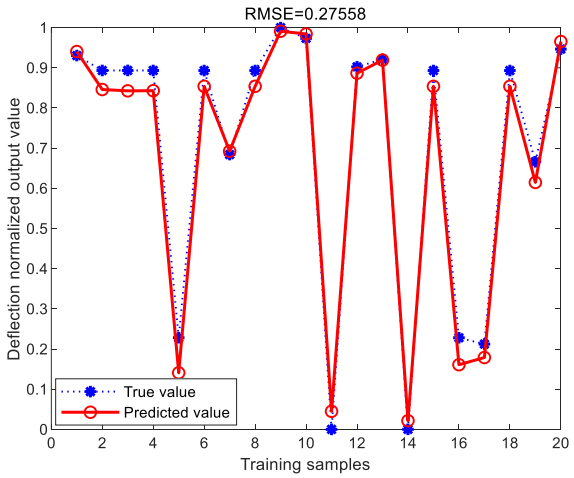

(a) Training samples of BP network

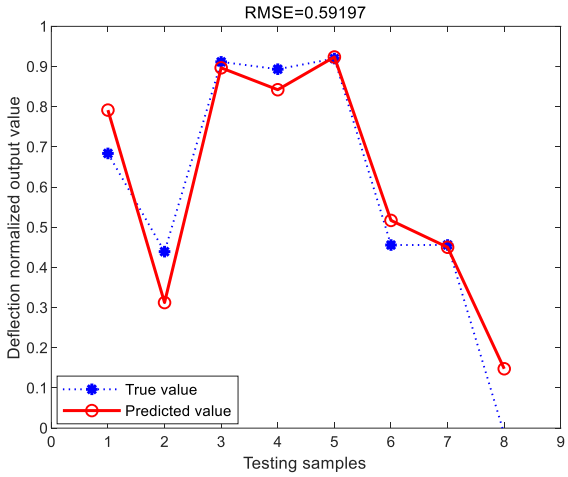

(b) Testing samples of BP network

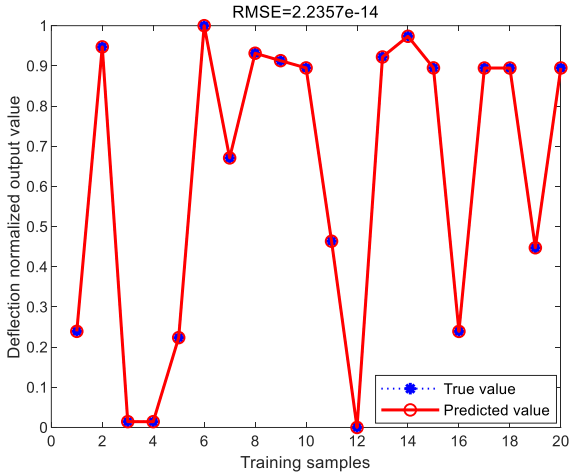

(c) Training samples of RBF network

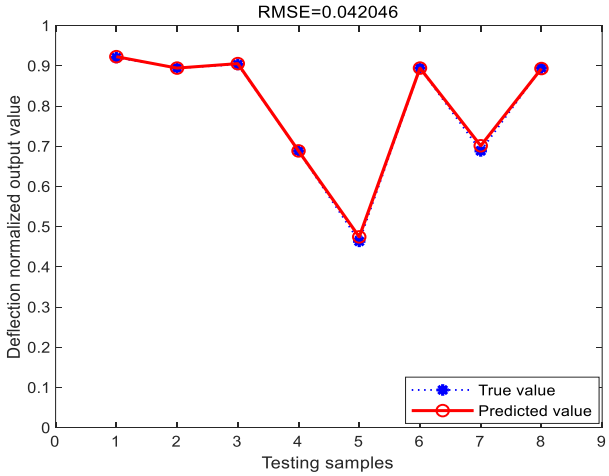

(d) Testing samples of RBF network

Fig. 6 The deflection prediction curves of the BP and RBF neural networks

By comparing the deflection values of the Midas/Civil finite element model with the measured values on site after the completion of the pouring and post-tensioning of pier segment 12 in pier 18, as shown in Table 7, it can be concluded that the model has good predictive capability.

Tab. 7 - Comparison table of model values and measured values

Construction phase	Deflection values of the model/m	Measured deflection values/m	Error/m	Relative error/%
Completion of pouring for pier segment 12 of pier 18.	3.464 x10^{-2}	3.500 x10^{-2}	3.600 x10^{-4}	1.03%
Completion of post-tensioning for pier segment 12 of pier 18.	2.551 x10^{-2}	2.670 x10^{-2}	1.190 x10^{-3}	4.45%

The prediction error of the neural network model reveals the model's precision. To more intuitively illustrate the difference between the predicted value and the actual value in the test sample, the original quantity scale of the data is restored using the inverse normalization function, and the prediction error and relative error of the two network prediction models are computed.

$$Error = Ri - Pi \quad (3)$$

$$Relative\ error = (Ri - Pi)/\ Ri \quad (4)$$

Where Ri is the true value; Pi is the predicted value.

According to Figure 7, The prediction error of the BP neural network model varies from 4 x10^{-5} m to 4.5 x10^{-4} m, with a maximum error of 4.1 x10^{-4} m and a maximum relative error of 1.6%; the prediction error of the RBF neural network model extends from 2 x10^{-5} m to 2.5 x10^{-4} m, with a maximum error of 2.3 x10^{-4} m and a maximum relative error of 1%. In the third round of test samples, both BP and RBF neural networks exhibit higher mistakes. For other groups of test data, RBF neural networks have prediction errors ranging between 2 x10^{-5} m to 2 x10^{-4} m, and their prediction performance is clearly superior to that of BP neural networks. Compared to the BP model, the RBF model provides greater prediction accuracy and greater stability.

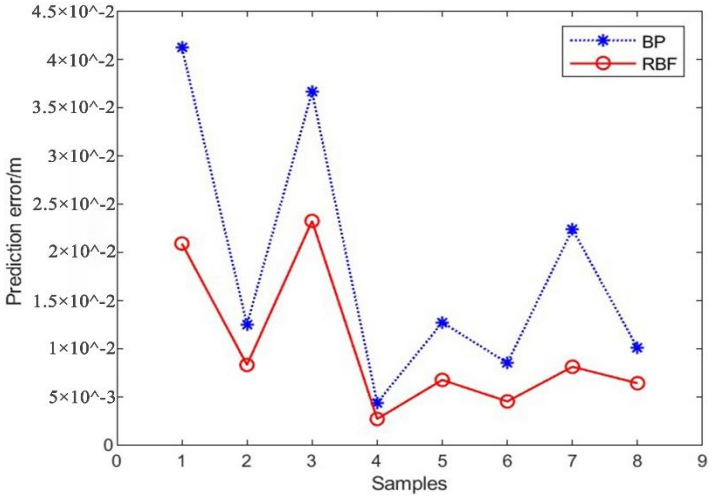

(a) Prediction error

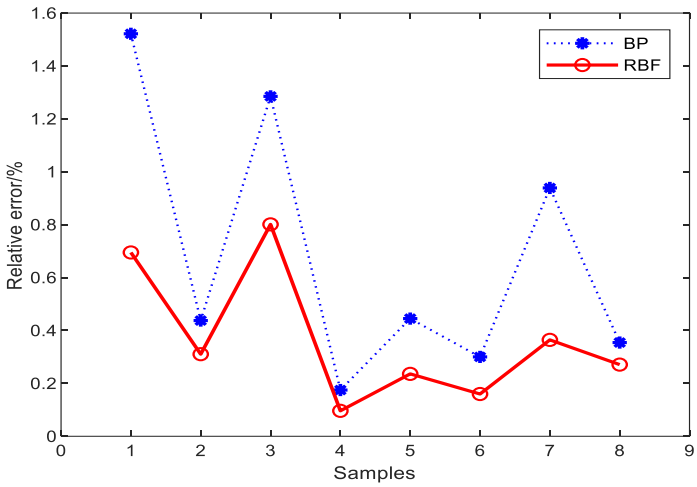

(b) Relative error

Fig. 7 - Error analysis of BP and RBF neural networks

The accuracy of the prediction model is measured using the mean absolute error (MAE) by comparing the predicted values to the actual values. The MAE of the BP model for the training sample is 2.117 x10^{-4} m, while the MAE for the test sample is 6.551 x10^{-4} m; the MAE of the RBF model for the training sample is 1.6x10^{-17} m, and the MAE for the test sample is 2.55 x10^{-5} m; both models demonstrate excellent prediction performance. The average absolute error of the RBF model on training and test samples is less than that of the BP model, and the RBF model has a smaller deviation between training and test samples, indicating that the RBF neural network model has superior generalization ability and prediction effect.

CONCLUSION

This research examines the effect of elastic modulus, volume weight of concrete, material age, and temperature load on the deflection of a rigid frame-continuous beam bridge, using measured values from the building site to fit the deflection curve with the average deflection technique. Four major parameters constitute input variables, while deflection is an output variable. Using MATLAB, the BP and RBF neural network methods are implemented to predict the deflection of the rigid frame-continuous beam bridge, and the following conclusions are drawn.

(1) Based on the principle of least squares and using the average deflection method, fit the deflection curve function at 1/4L of Pier 18 of the supporting structure from late August 2022 to early January 2023, $f = 0.00929t^3 - 0.1725\ t^2 + 0.01547\ t - 1.186$, based on the Least Squares Principle, and its accuracy was confirmed. The Average Deflection Method can be used to fit and predict the average deflection value over a longer time period and the average deflection value over the next longer time period.

(2) The prediction models established by the RBF neural network and the BP neural network have a high fitting correlation coefficient under the same conditions, and both neural networks can accurately predict the deflection values under various influencing parameters, providing a basis for the selection of influencing parameters.

(3) Comparing the prediction models of RBF neural network and BP neural network reveals that RBF neural network is more stable; the average absolute error of training samples is 1.6x10^{-17} m, whereas the average absolute error of test samples is 2.55 x10^{-5} m; the generalization ability of the model is superior; the training is more stable; and the prediction effect is superior.

(4) Comparing the prediction models of the RBF neural network and the BP neural network, it was discovered that the prediction error of the RBF neural network model ranged from 2 x10^{-5} m to 2.5 x10^{-4} m, with a maximum error of 2.3 x10^{-4} m and a relative error that did not exceed 1%. Clearly,

the prediction performance was superior to that of the BP neural network. Compared to the BP model, the RBF model has greater prediction accuracy and greater stability.

ACKNOWLEDGEMENTS

The research in this paper was supported by the guidance project of the key R&D program of Heilongjiang Province Grant (No. GZ20220133).

REFERENCES

[1] Editorial Department of China Journal of Highway and Transport, 2021. 'Review on China's Bridge Engineering Research:2021', China Journal of Highway and Transport, vol. 34(02):1-97. doi. 10.19721/j.cnki.1001-7372.2021.02.001
[2] Meng Lingxing, 2008. Research on Construction Control of Long-span Prestressed Continuous Rigid Frame Bridge. Master 's degree thesis of Shandong University.
[3] Yuan Zengren, 1999. Artificial Neural Networks and Its Applications, Tsinghua University Press.
[4] Jiang Zongli, 2001. Introduction to Artificial Neural Network, Higher Education Press.
[5] Yan Pingfan, Zhang Changshui, 2005. Artificial Neural Networks and Simulated Evolutionary Computation, Tsinghua University Press.
[6] Hou Yuanbin, Du Jingyi, Wang Mei, 2007. Neural Network, Xi 'an University of Electronic Science and Technology Press.
[7] Chen Ming, 2013. Principles and Examples of MATLAB Neural Networks, Tsinghua University Press.
[8] Liu Xiaoyao, Xu Yue, 2011. Design Manual for Highway Bridges and Culverts: Beam Bridges (2nd Edition), China Communications Press.
[9] Sun Quansheng, Wu Tong, 2010. Application of BP Neural Network in the Cable-replacing Construction Control of Cable-stayed Bridge, China Safety Science Journal, vol. 2010,20(07):21-25. doi. 10.16265/j.cnki.issn1003-3033.2010.07.012
[10] Peng Binbin, Yan Xianguo, Du Juan, 2020. Research on Surface Quality Prediction Based on BP and RBF Neural Network, Surface Technology, vol. 2020,49(10):324-328,337. doi.10.16490/j.cnki.issn.1001-3660.2020.10.038
[11] Wang Ting, 2019. Study on mathematical model and fractal properties of porosity of electrospun nanofiber membrane, Tiangong University.
[12] Kang Le, Liu Yuankun, Wang Liping, Gao Xiaoping, 2021. Preparation of electrospun nanofiber membrane for air filtration and process optimization based on BP neural network, Materials Research Express, vol. 2021,8(11):115010. doi.10.1088/2053-1591/ac37d6
[13] Kang Le, Wang Lizhi, GAO Xiaoping, 2022. Process optimization of polyvinylidene fluoride/polypropylene gradient composite filter material based on BP neural network, Acta Materiae Compositae Sinica, vol. 2022, 39(08):3776-3785. doi.10.13801/j.cnki.fhclxb.20210913.005
[14] Zhou Jinhua, Ren Junxue, Cai Ju, 2018. Prediction of milling residual stress of aviation blade based on RBF neural network, Computer Integrated Manufacturing Systems, vol. 2018, 24(02):361-370. doi. 10.13196/j.cims.2018.02.008
[15] Tao Jili, Yu Zheng, Zhang Ridong, Gao Furong, 2021. RBF neural network modeling approach using PCA based LM–GA optimization for coke furnace system, Applied Soft Computing, 111:1076. doi. 10.1016/j.asoc.2021.107691
[16] Feng Jianhu, Che Gangming, Nie Yufeng, 2006. Numerical Analysis Principles, Science Press.
[17] Hossein Mohammad Khanlou, Ali Sadollah, Bee Chin Ang, et al, 2014. Prediction and optimization of electrospinning parameters for polymethyl methacrylate nanofiber fabrication using response surface methodology and artificial neural networks, Neural Computing and Applications, vol. 2014, 25(03):767-777. doi. 10.1007/s00521-014-1554-8
[18] Komeil Nasouri, Hossein Bahrambeygi, Amir Rabbi, et al, 2012. Modeling and optimization of electrospun PAN nanofiber diameterusing response surface methodology and artificial neural networks, Journal of Applied Polymer Science, vol. 2012, 126(01):127-135. doi. 10.1002/app.36726
[19] Lei Junqing, 2009. Analysis of deflection causes of long-span prestressed concrete continuous rigid frame bridge, Master Degree Thesis of Beijing Jiaotong University.
[20] Zhan Jianhui, Chen Hui, 2005. Cause analysis of main beam deflection and box girder crack of large span continuous rigid frame, Journal of China & Foreign Highway, vol. 2005, 25(01):56-58. doi. 10.14048/j.issn.1671-2579.2005.01.015

[21] Li Qiao, Bu Yizhi, Zhang Qinghua, 2009. Whole-procedure adaptive construction control system based on geometry control method, CHINA CIVIL ENDINEERING JOURNAL, vol. 2009, 42(07):69-77. doi. 10.15951/j.tmgcxb.2009.07.014
[22] Xing Yun, Wu Xun, 2007. Study on the Excessive Long-Term Deflection of Large Span Prestressed Concrete Girder Bridges, Structural Engineers. doi. 10.15935/j.cnki.jggcs.2007.05.003
[23] Li YunXi, Liu Yongjian, 2008. Study on the Influence Factors of Long-term Deflection for Prestressed Concrete Continuous Box-girder Bridge. Modern Transportation Technology, vol. 2008, 05(05).
[24] Xie Jun, Wang Guoliang, Zheng Xiaohua, 2007. State of Art of Long-term Deflection for Long Span Prestressed Concrete Box-girder Bridge. Journal Highway and Transportation Research and Development, vol. 2007, 24(01):47-50.
[25] Wang Fei, 2007. Construction monitoring and shrinkage and creep effect analysis of continuous rigid frame bridge, Master Degree Thesis of Beijing Jiaotong University.
[26] Vitek J.L, 1997. Long-term deflections of large prestressed concrete bridg, Progress Report CEB Bulletin, No235.
[27] Pan Z, Fu C.C, Lu Z, 2010. Impact of longitudinal tendons on long-term deflections oflong-span concrete cantilever bridges, Bridge Maintenance, Safety, Management and Life-Cycle Optimization-Proceedings of the 5th International Conference on Bridge Maintenance, Safety and Management. Philadelphia, PA, United states. doi. 10.1201/b10430-349
[28] Piotr Gwoździewicz, Bruno Jurkiewiez, Jean-François Destrebecq, 2000. Long Term Serviceability of Concrete Structures with Regards to Material Behaviors and Cyclic Loading, Proceedings of the 2000 Structures Congress-Advanced Technology in Structural Engineering, Philadelphia Pennsylvania USA:ASCE. doi. 10.1061/40492(2000)159
[29] Huang Zhongwen, 2011. Research on reducing deflection technology of long-span prestressed concrete beam bridge, Engineering Master's thesis of Chongqing Jiaotong University.
[30] Cao Qingsong, Zhou Jihui, 2004. Application of MATLAB in Neural Network Design, JOURNAL Of EAST CHINA JIAOTONG UNIVERSITY, vol. 2004, 21(04):86-88.
[31] Li Qiaoru, Liu Guixin, Chen Liang, et al, 2023. Short-term traffic flow prediction based on adaptive BAS optimized RBF neural network, Journal of Harbin Institute of Technology, vol. 2023, 55(03):93-99. doi. 10.11918 /202108096